Seismic ambient noise modeling for Lausitz ET candidate site

Shi Yao[1,4,5], Yajian Gao[1], Mike Lindner[2,3], Andreas Rietbrock[1]

1 Geophysical Institute, Karlsruhe Institute of Technology 2 Deutsches Elektronen-Synchrotron DESY
3 Deutsche Zentrum für Astrophysik DZA 4 Institute of Geology and Geophysics 5 University of Chinese Academy of Sciences

Introduction

- 2D and 3D seismic simulations are conducted for the Lausitz region by solving seismic viscoelastic wave equation using Spectral Element Method (SEM).
- Effects of topography and loose sedimentary structures are investigated through simulations using different models and recordings at multiple locations.
- Ambient noise field are simulated using Green's function (solution to the wave equation with a delta function as the source term) library and randomly distributed noise sources with randomly perturbed phase shifts.
- Probabilistic Power Spectral Density (PPSD) of synthetic ambient noise are calculated.
- P-wave and S-wave displacements are extracted from the wavefields and can be used to calculate density fluctuations.

Methodology

$$\rho \partial_t^2 \boldsymbol{u} = \nabla \cdot \boldsymbol{\sigma} + \boldsymbol{f}$$

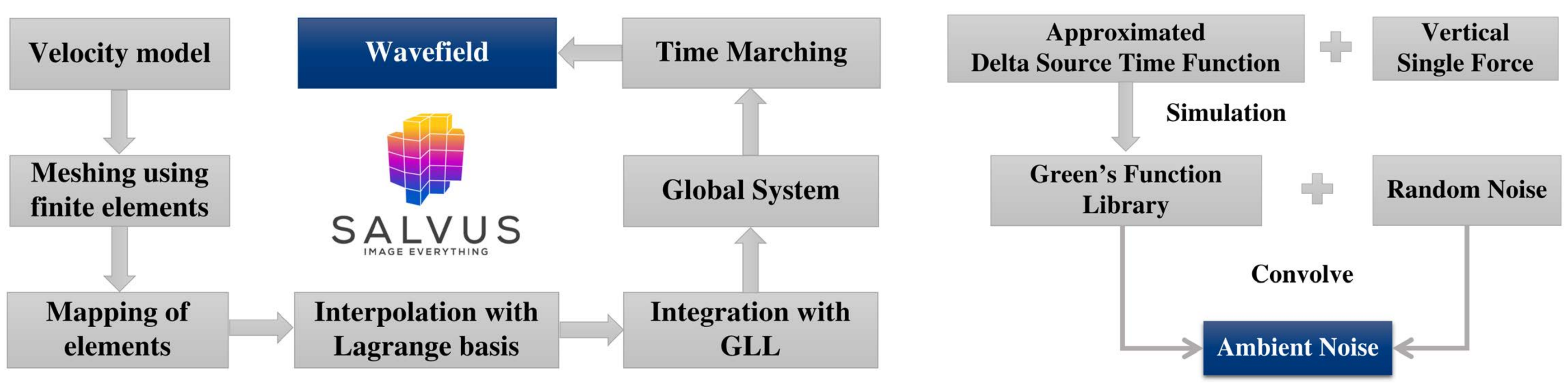

Fig. 1 (a) SEM simulation workflow and (b) ambient noise simulation workflow.

Exploring the Effects of Sediment in 2D Simulations

Simulation Settings

$$\mathbf{f} = (0, 0, f\hat{\mathbf{z}})$$

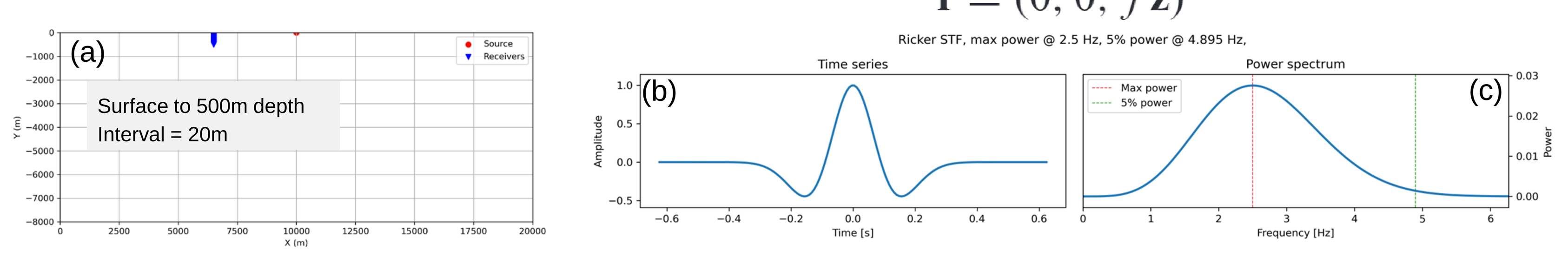

Fig. 2 (a) Spatial distribution of sources and receivers. (b) Ricker wavelet in the time domain. (c) Power spectrum of the Ricker wavelet.

Homogeneous Model

Fig. 3 (a) Wavefield snapshot at t = 2 s. (b) Wavefield snapshot at t = 3.5 s. (c) Seismic waveforms recorded at different locations. (d) Amplitude ratio between buried and surface stations as a function of burial depth.

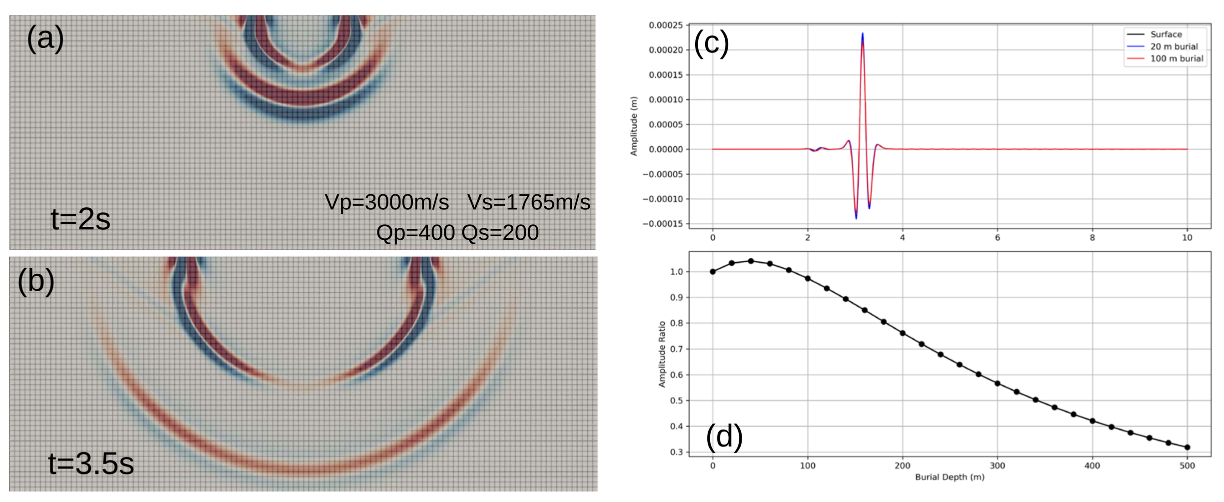

Loose-sediment Model

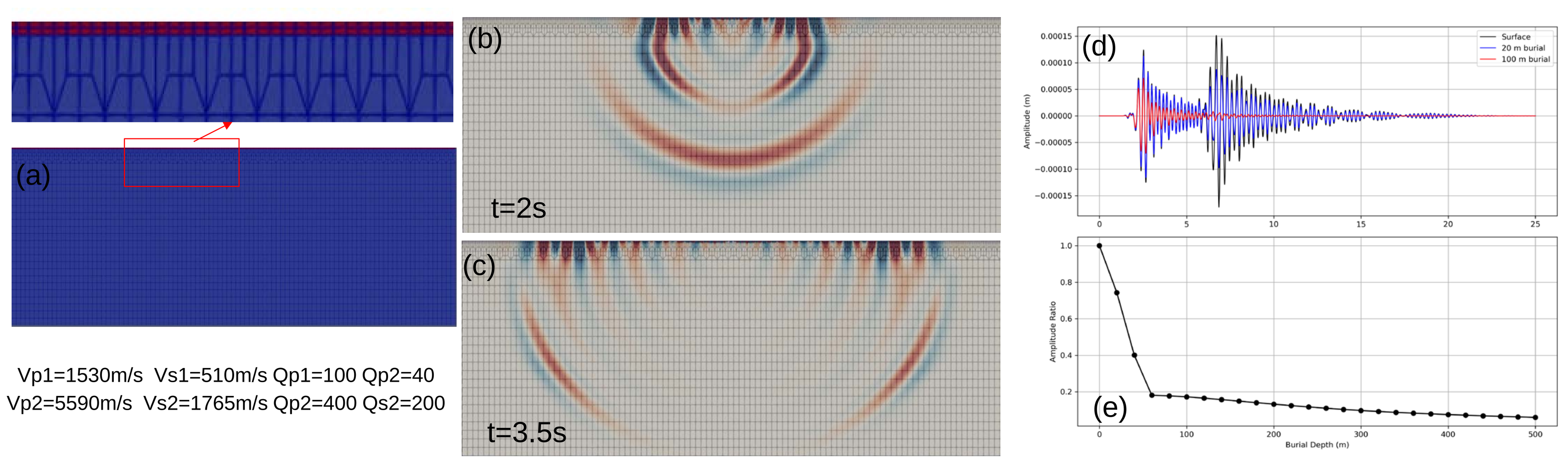

Fig. 4 (a) P-wave velocity model overlaid with the computational mesh. (b) Wavefield snapshot at t = 2 s. (c) Wavefield snapshot at t = 8s. (d) Seismic waveforms recorded at different locations. (e) Amplitude ratio between buried and surface stations.

Wavefield Separation

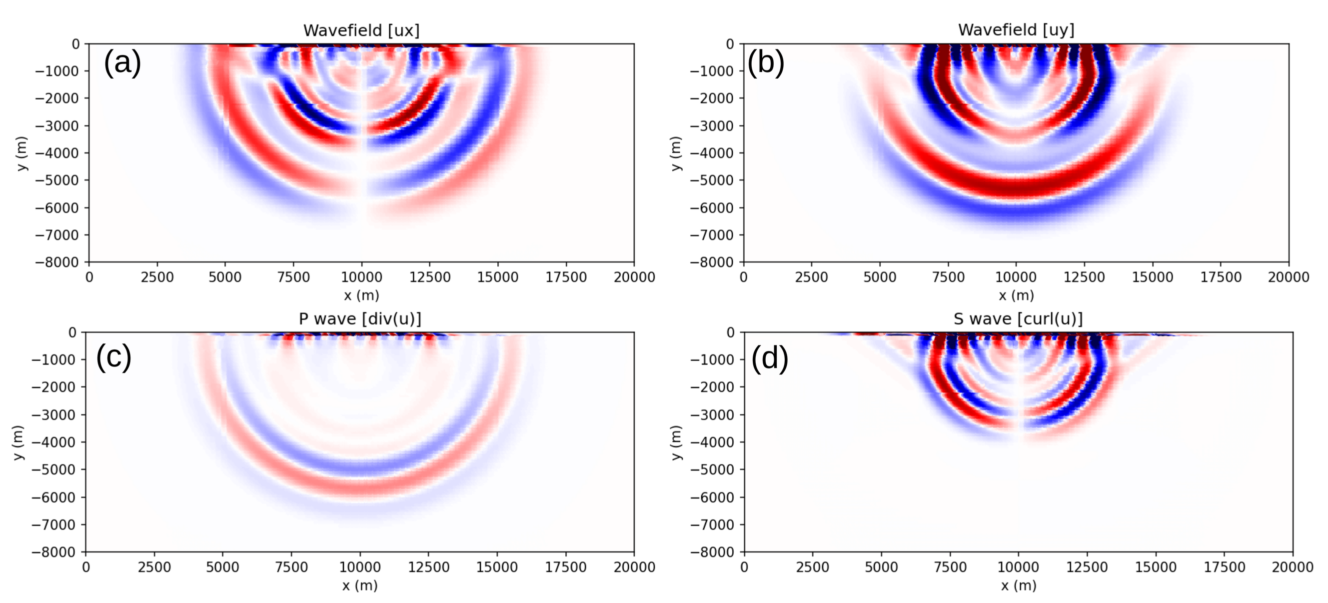

Fig. 5 Wavefield snapshots at t=2s. (a) X-component of displacement. (b) Y-component of displacement. (c) Divergence of the displacement field. (d) Curl of the displacement field.

3D Topography Scatterings

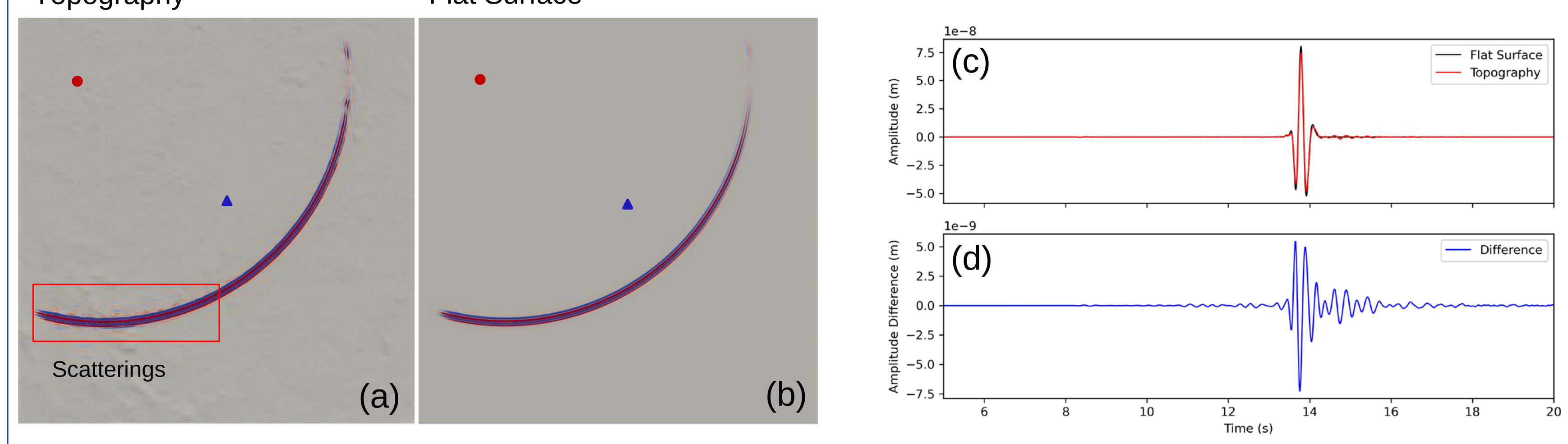

Fig. 6 (a) Snapshot of the wavefield in the topography model. (b) Snapshot of the wavefield in the flat surface model. (c) Comparison of waveforms recorded in the flat surface and topography models. (d) Waveform differences between the two models.

Ambient Noise Simulation

- Simulation Settings

$$\mathbf{f} = (0, 0, f\hat{\mathbf{z}})$$

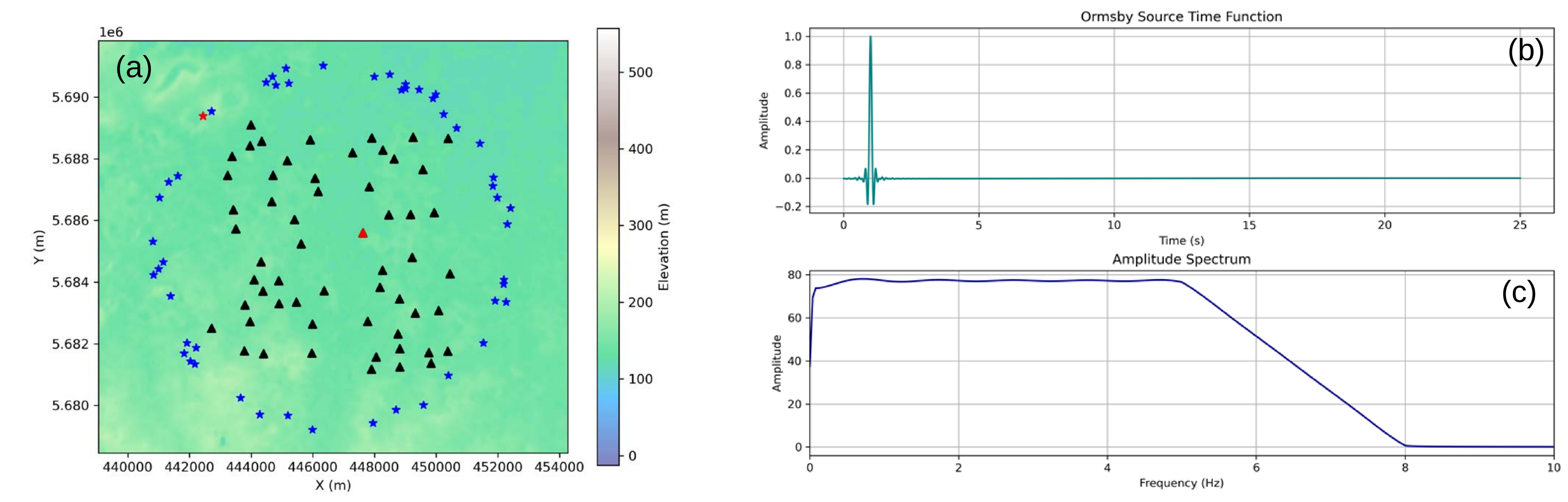

Fig. 7 (a) Spatial distribution of sources and receivers. (b) Ormsby wavelet in the time domain. (c) Power spectrum of the Ormsby wavelet.

- Noise Generation

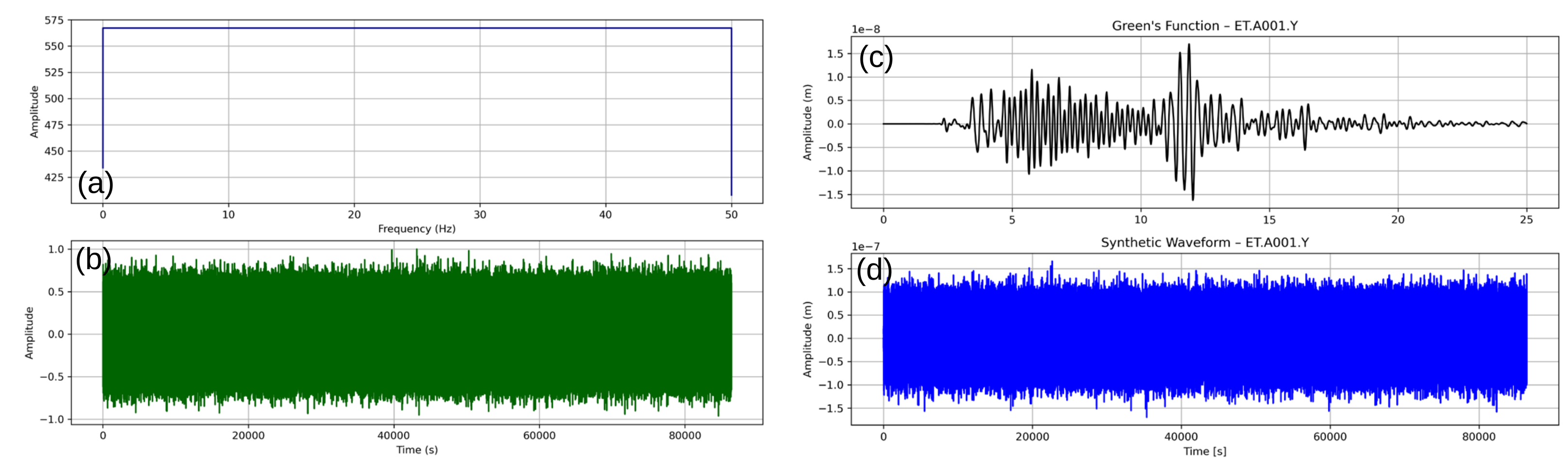

Fig. 8 (a) Amplitude spectrum of the random noise. (b) Random noise signal in the time domain. (c) Green's function obtained from numerical simulation. (d) Synthetic ambient noise generated by convolving the random noise with the Green's function.

- Mean Probabilistic Power Spectral Density (PPSD)

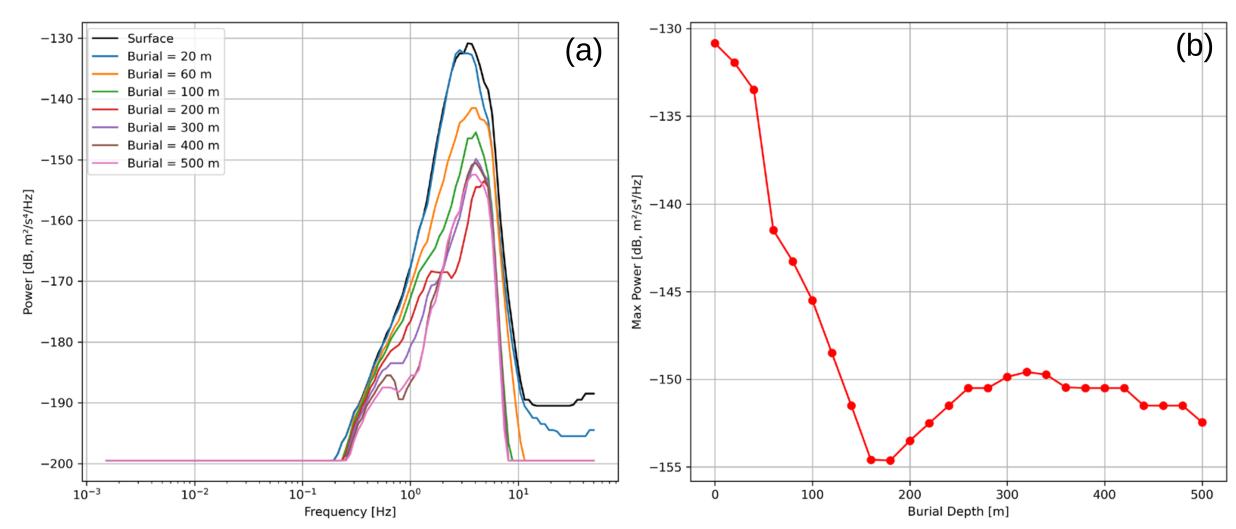

Fig. 9 (a) Mean PPSDs of waveforms recorded at different locations. (b) Maximum of mean PPSD of surface and buried stations.

Conclusion and Outlook

- The low-velocity, high-attenuation loose sediments significantly affect the waveforms, as the energy becomes trapped within the sediment layer. As a result, the amplitude of the recordings above the sediment interface is much stronger.
- The topography can introduce slightly scatterings, but will not affect too much on the waveforms.
- The displacement divergence of any given model can be computed, which can be used to predict fluctuations in density, we will extend it to 3D simulations in further steps.

References

[1] Afanasiev M, Boehm C, van Driel M, et al. Modular and flexible spectral-element waveform modelling in two and three dimensions[J]. Geophysical Journal International, 2019, 216(3): 1675-1692.

[2] van Driel M, Nissen-Meyer T. Optimized viscoelastic wave propagation for weakly dissipative media[J]. Geophysical Journal International, 2014, 199(2): 1078-1093.

[3] Zhou X Y, Chang X, Wang Y B, et al. Non-artifact vector P-and S-wave separation for elastic reverse time migration[J]. Petroleum Science, 2022, 19(6): 2695-2710.

Acknowledgement

This work was carried out as part of the ET-GEO project funded by BMBF. We acknowledge the Earth System Modelling Project (ESM) for funding this work by providing computing time on the ESM partition of the supercomputer JUWELS (Jülich Supercomputing Centre, 2021) at the Jülich Supercomputing Centre (JSC). We also acknowledge Dresden University for providing computing resources.

Contact:
shi.yao@partner.kit.edu
andreas.rietbrock@kit.edu